

Experimental Constraints on the Spin and Parity of the $\Lambda_c(2880)^+$

R. Mizuk,¹² K. Abe,⁷ I. Adachi,⁷ H. Aihara,⁴⁵ D. Anipko,¹ V. Aulchenko,¹ T. Aushev,^{17,12} A. M. Bakich,⁴⁰ V. Balagura,¹² E. Barberio,²⁰ A. Bay,¹⁷ I. Bedny,¹ K. Belous,¹¹ U. Bitenc,¹³ I. Bizjak,¹³ S. Blyth,²³ A. Bondar,¹ A. Bozek,²⁶ M. Bračko,^{7,19,13} J. Brodzicka,²⁶ T. E. Browder,⁶ M.-C. Chang,³ A. Chen,²³ K.-F. Chen,²⁵ W. T. Chen,²³ B. G. Cheon,⁵ R. Chistov,¹² Y. Choi,³⁹ Y. K. Choi,³⁹ S. Cole,⁴⁰ J. Dalseno,²⁰ M. Danilov,¹² A. Drutskoy,² S. Eidelman,¹ D. Epifanov,¹ S. Fratina,¹³ N. Gabyshev,¹ A. Garmash,³⁴ T. Gershon,⁷ G. Gokhroo,⁴¹ B. Golob,^{18,13} H. Ha,¹⁵ J. Haba,⁷ K. Hayasaka,²¹ H. Hayashii,²² M. Hazumi,⁷ D. Heffernan,³¹ T. Hokuue,²¹ Y. Hoshi,⁴³ S. Hou,²³ W.-S. Hou,²⁵ T. Iijima,²¹ K. Ikado,²¹ A. Imoto,²² K. Inami,²¹ A. Ishikawa,⁴⁵ R. Itoh,⁷ M. Iwasaki,⁴⁵ Y. Iwasaki,⁷ H. Kaji,²¹ J. H. Kang,⁴⁹ P. Kapusta,²⁶ N. Katayama,⁷ H. R. Khan,⁴⁶ H. Kichimi,⁷ Y. J. Kim,⁴ K. Kinoshita,² S. Korpar,^{19,13} P. Križan,^{18,13} P. Krokovny,⁷ R. Kulasiri,² R. Kumar,³² C. C. Kuo,²³ A. Kuzmin,¹ Y.-J. Kwon,⁴⁹ G. Leder,¹⁰ J. Lee,³⁷ M. J. Lee,³⁷ S. E. Lee,³⁷ T. Lesiak,²⁶ S.-W. Lin,²⁵ D. Liventsev,¹² G. Majumder,⁴¹ F. Mandl,¹⁰ T. Matsumoto,⁴⁷ A. Matyja,²⁶ S. McOnie,⁴⁰ H. Miyake,³¹ H. Miyata,²⁸ Y. Miyazaki,²¹ M. Nakao,⁷ Z. Natkaniec,²⁶ S. Nishida,⁷ S. Ogawa,⁴² T. Ohshima,²¹ S. Okuno,¹⁴ Y. Onuki,³⁵ H. Ozaki,⁷ P. Pakhlov,¹² G. Pakhlova,¹² H. Park,¹⁶ K. S. Park,³⁹ L. S. Peak,⁴⁰ R. Pestotnik,¹³ L. E. Piilonen,⁴⁸ Y. Sakai,⁷ N. Satoyama,³⁸ O. Schneider,¹⁷ J. Schümann,²⁴ R. Seidl,^{8,35} K. Senyo,²¹ M. E. Sevier,²⁰ M. Shapkin,¹¹ H. Shibuya,⁴² J. B. Singh,³² A. Somov,² N. Soni,³² S. Stanič,²⁹ M. Starič,¹³ H. Stoeck,⁴⁰ S. Y. Suzuki,⁷ F. Takasaki,⁷ K. Tamai,⁷ M. Tanaka,⁷ G. N. Taylor,²⁰ Y. Teramoto,³⁰ X. C. Tian,³³ I. Tikhomirov,¹² T. Tsuboyama,⁷ T. Tsukamoto,⁷ S. Uehara,⁷ T. Uglov,¹² K. Ueno,²⁵ S. Uno,⁷ P. Urquijo,²⁰ Y. Usov,¹ G. Varner,⁶ S. Villa,¹⁷ C. H. Wang,²⁴ Y. Watanabe,⁴⁶ E. Won,¹⁵ Q. L. Xie,⁹ B. D. Yabsley,⁴⁰ A. Yamaguchi,⁴⁴ Y. Yamashita,²⁷ M. Yamauchi,⁷ C. Z. Yuan,⁹ L. M. Zhang,³⁶ Z. P. Zhang,³⁶ V. Zhilich,¹ and A. Zupanc¹³

(Belle Collaboration)

¹*Budker Institute of Nuclear Physics, Novosibirsk*

²*University of Cincinnati, Cincinnati, Ohio 45221*

³*Department of Physics, Fu Jen Catholic University, Taipei*

⁴*The Graduate University for Advanced Studies, Hayama, Japan*

⁵*Hanyang University, Seoul*

⁶*University of Hawaii, Honolulu, Hawaii 96822*

⁷*High Energy Accelerator Research Organization (KEK), Tsukuba*

⁸*University of Illinois at Urbana-Champaign, Urbana, Illinois 61801*

⁹*Institute of High Energy Physics, Chinese Academy of Sciences, Beijing*

¹⁰*Institute of High Energy Physics, Vienna*

¹¹*Institute of High Energy Physics, Protvino*

¹²*Institute for Theoretical and Experimental Physics, Moscow*

¹³*J. Stefan Institute, Ljubljana*

¹⁴*Kanagawa University, Yokohama*

¹⁵*Korea University, Seoul*

¹⁶*Kyungpook National University, Taegu*

¹⁷*Swiss Federal Institute of Technology of Lausanne, EPFL, Lausanne*

¹⁸*University of Ljubljana, Ljubljana*

¹⁹*University of Maribor, Maribor*

²⁰*University of Melbourne, Victoria*

²¹*Nagoya University, Nagoya*

²²*Nara Women's University, Nara*

²³*National Central University, Chung-li*

²⁴*National United University, Miao Li*

²⁵*Department of Physics, National Taiwan University, Taipei*

²⁶*H. Niewodniczanski Institute of Nuclear Physics, Krakow*

²⁷*Nippon Dental University, Niigata*

²⁸*Niigata University, Niigata*

²⁹*University of Nova Gorica, Nova Gorica*

³⁰*Osaka City University, Osaka*

³¹*Osaka University, Osaka*

³²*Panjab University, Chandigarh*

³³*Peking University, Beijing*

³⁴*Princeton University, Princeton, New Jersey 08544*³⁵*RIKEN BNL Research Center, Upton, New York 11973*³⁶*University of Science and Technology of China, Hefei*³⁷*Seoul National University, Seoul*³⁸*Shinshu University, Nagano*³⁹*Sungkyunkwan University, Suwon*⁴⁰*University of Sydney, Sydney NSW*⁴¹*Tata Institute of Fundamental Research, Bombay*⁴²*Toho University, Funabashi*⁴³*Tohoku Gakuin University, Tagajo*⁴⁴*Tohoku University, Sendai*⁴⁵*Department of Physics, University of Tokyo, Tokyo*⁴⁶*Tokyo Institute of Technology, Tokyo*⁴⁷*Tokyo Metropolitan University, Tokyo*⁴⁸*Virginia Polytechnic Institute and State University, Blacksburg, Virginia 24061*⁴⁹*Yonsei University, Seoul*

(Received 12 January 2007; published 28 June 2007)

We report the results of several studies of the $\Lambda_c^+ \pi^+ \pi^- X$ final state in continuum $e^+ e^-$ annihilation data collected by the Belle detector. An analysis of angular distributions in $\Lambda_c(2880)^+ \rightarrow \Sigma_c(2455)^{0,++} \pi^{+,-}$ decays strongly favors a $\Lambda_c(2880)^+$ spin assignment of $\frac{5}{2}$ over $\frac{3}{2}$ or $\frac{1}{2}$. We find evidence for $\Lambda_c(2880)^+ \rightarrow \Sigma_c(2520)^{0,++} \pi^{+,-}$ decay and measure the ratio of $\Lambda_c(2880)^+$ partial widths $\Gamma(\Sigma_c(2520)\pi)/\Gamma(\Sigma_c(2455)\pi) = 0.225 \pm 0.062 \pm 0.025$. This value favors the $\Lambda_c(2880)^+$ spin-parity assignment of $\frac{5}{2}^+$ over $\frac{3}{2}^-$. We also report the first observation of $\Lambda_c(2940)^+ \rightarrow \Sigma_c(2455)^{0,++} \pi^{+,-}$ decay and measure $\Lambda_c(2880)^+$ and $\Lambda_c(2940)^+$ mass and width parameters. These studies are based on a 553 fb^{-1} data sample collected at or near the $\Upsilon(4S)$ resonance at the KEKB collider.

DOI: 10.1103/PhysRevLett.98.262001

PACS numbers: 14.20.Lq, 13.30.Eg

Charmed baryon spectroscopy provides an excellent laboratory to study the dynamics of a light diquark in the environment of a heavy quark, allowing the predictions of different theoretical approaches to be tested [1–4]. There are 12 experimentally observed charmed baryons for which the spins and parities are assigned [5,6]. They include ground states, spin excitations, and lowest orbital excitations. Except for the Λ_c^+ , the J^P quantum numbers for these states have not been determined experimentally but are instead assigned based on the quark model predictions for their masses. There are also six charmed baryons, recently observed at the CLEO [7], Belle [8,9], and BABAR [10] experiments, for which the spins and parities are not well constrained. The new states are in a mass region where the quark model predicts many levels with small spacing, which makes the J^P assignment difficult. In this Letter we investigate possible spin and parity values of one such state, the $\Lambda_c(2880)^+$ baryon [7,10], by studying the resonant structure of $\Lambda_c(2880)^+ \rightarrow \Lambda_c^+ \pi^+ \pi^-$ decays and performing an angular analysis of $\Lambda_c(2880)^+ \rightarrow \Sigma_c(2455)^{0,++} \pi^{+,-}$ decays. We also report the first observation of $\Lambda_c(2940)^+ \rightarrow \Sigma_c(2455)^{0,++} \pi^{+,-}$ decay and measure $\Lambda_c(2880)^+$ and $\Lambda_c(2940)^+$ mass and width parameters.

We use a 553 fb^{-1} data sample collected with the Belle detector at or 60 MeV below the $\Upsilon(4S)$ resonance, at the KEKB asymmetric-energy (3.5 GeV on 8.0 GeV) $e^+ e^-$

collider [11]. The Belle detector [12] is a large-solid-angle magnetic spectrometer that consists of a silicon vertex detector, a 50-layer cylindrical drift chamber, an array of aerogel threshold Cherenkov counters, a barrel-like array of time-of-flight scintillation counters, and an array of CsI(Tl) crystals located inside a superconducting solenoidal coil that produces a 1.5 T magnetic field. An iron flux return located outside the coil is instrumented to detect muons and K_L^0 mesons. We use a GEANT based Monte Carlo (MC) simulation [13] to model the response of the detector and to determine its acceptance. Signal MC events are generated with experimental run dependence in proportion to the relative luminosities of different running periods.

Λ_c^+ baryons are reconstructed using the $pK^- \pi^+$ decay mode (the inclusion of charge conjugate modes is implied throughout this Letter). To select proton, charged kaon and pion candidates we use the same track quality and particle identification criteria as for observation of the $\Sigma_c(2800)$ isotriplet [8]. The invariant mass of the $pK^- \pi^+$ combination is required to be within $\pm 8 \text{ MeV}/c^2$ (1.6σ) of the Λ_c^+ mass value, recently measured by BABAR [14]. To improve the accuracy of the Λ_c^+ momentum measurement, we perform a mass constrained fit to the $pK^- \pi^+$ vertex. We combine Λ_c^+ candidates with the remaining $\pi^+ \pi^-$ candidates in the event. To reduce the combinatorial background, we impose a requirement on the scaled

momentum of the $\Lambda_c^+ \pi^+ \pi^-$ combination $x_p \equiv p^*/\sqrt{E_{\text{beam}}^{*2} - M^2} > 0.7$, where p^* is the momentum and M is the invariant mass of the combination, E_{beam}^* is the beam energy, with all variables being measured in the center-of-mass frame. The high x_p requirement is justified by the high-peaked momentum spectra of known excited charmed baryons. To improve the $M(\Lambda_c^+ \pi^+ \pi^-)$ resolution we perform an interaction point constrained fit to the $\Lambda_c^+ \pi^+ \pi^-$ vertex.

To measure the $\Lambda_c(2880)^+$ mass and width, we apply an additional requirement that either $M(\Lambda_c^+ \pi^-)$ or $M(\Lambda_c^+ \pi^+)$ be in the $\Sigma_c(2455)$ signal region defined as $2450 < M < 2458 \text{ MeV}/c^2$. Whereas 35% of signal events pass this cut, only 12% of background events do so. From MC simulation we find that the mass resolution for the $\Lambda_c(2880)^+ \rightarrow \Sigma_c(2455)^{0,++} \pi^{+,-}$ decays depends strongly on the decay angle θ , defined as the angle between the pion momentum in the $\Lambda_c(2880)^+$ rest frame and the boost direction of the $\Lambda_c(2880)^+$. To assure good resolution for the $\Lambda_c(2880)^+$ mass and width measurement we require $\cos\theta > 0$. This requirement also helps to suppress combinatorial background. The resulting $M(\Lambda_c^+ \pi^+ \pi^-)$ distribution is shown in Fig. 1. One can see clear peaks from the $\Lambda_c(2765)^+$ and $\Lambda_c(2880)^+$. A peak in the region $M = 2940 \text{ MeV}/c^2$ is associated with the $\Lambda_c(2940)^+$ baryon recently observed in the $D^0 p$ final state by BABAR [10]. Scaled $\Sigma_c(2455)$ sidebands, which are also shown in Fig. 1, are featureless in the

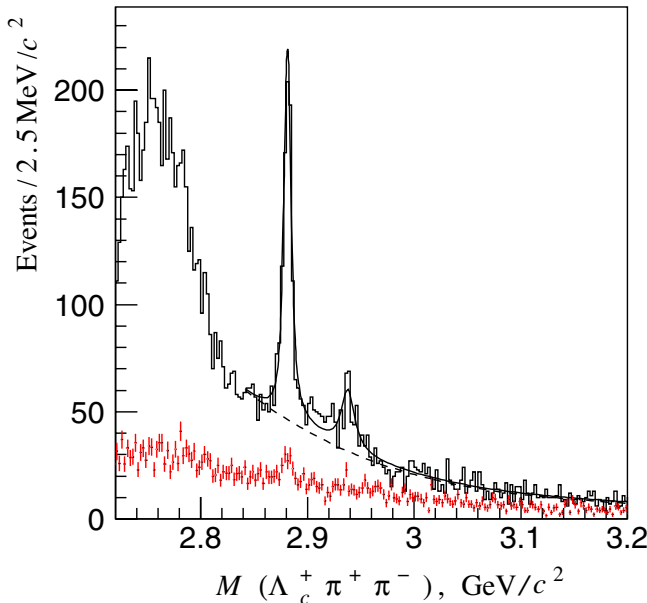


FIG. 1 (color online). The invariant mass of the $\Lambda_c^+ \pi^+ \pi^-$ combinations for the $\Sigma_c(2455)$ signal region (histogram) and scaled sidebands (dots with error bars). The fit result (solid curve) and its combinatorial component (dashed curve) are also presented.

region of the $\Lambda_c(2940)^+$. The $\Sigma_c(2455)$ sidebands are defined as $2438 < M(\Lambda_c^+ \pi) < 2446 \text{ MeV}/c^2$ and $2462 < M(\Lambda_c^+ \pi) < 2470 \text{ MeV}/c^2$.

We perform a binned likelihood fit to the $\Lambda_c^+ \pi^+ \pi^-$ mass spectrum of Fig. 1 to extract the mass and width parameters and yields of the $\Lambda_c(2880)^+$ and $\Lambda_c(2940)^+$. The fitting function is a sum of three components: $\Lambda_c(2880)^+$ signal, $\Lambda_c(2940)^+$ signal, and combinatorial background functions. As shown below, the spin-parity assignment favored for the $\Lambda_c(2880)^+$ is $\frac{5}{2}^+$; therefore, the $\Lambda_c(2880)^+$ signal is parametrized by an F -wave Breit-Wigner function convolved with the detector resolution function, determined from MC simulation ($\sigma = 2.2 \text{ MeV}/c^2$). The $\Lambda_c(2940)^+$ signal is an S -wave Breit-Wigner function convolved with the detector resolution function ($\sigma = 2.4 \text{ MeV}/c^2$). The background is parametrized by a third-order polynomial. We find that the results of the fit do not depend on the bin size b , if $b \leq 0.5 \text{ MeV}/c^2$. Therefore all fits to the $\Lambda_c^+ \pi^+ \pi^-$ mass spectra are performed for $b = 0.5 \text{ MeV}/c^2$. The fit is shown in Fig. 1, and the results are summarized in Table I. The signal yield is defined as the integral of the Breit-Wigner function over a $\pm 2.5\Gamma$ interval. The normalized χ^2 of the fit is $\chi^2/\text{d.o.f.} = 771.5/710$ (probability 5.4%). If the $\Lambda_c(2940)^+$ signal is removed from the fit, the double log likelihood changes by 59.8, which corresponds (for three degrees of freedom) to a signal significance of 7.2 standard deviations.

To estimate the systematic uncertainty on the results of the fit we vary the background parametrization, using a fourth-order polynomial and the inverse of a third-order polynomial. We include the $\Lambda_c(2765)^+$ signal region into the fit interval, parametrizing the $\Lambda_c(2765)^+$ signal by an S -wave Breit-Wigner function. The $\Lambda_c(2765)^+$ mass and width determined from the fit are $M = (2761 \pm 1) \text{ MeV}/c^2$ and $\Gamma = (73 \pm 5) \text{ MeV}$. We vary the selection requirements; we take into account the uncertainty in the Λ_c^+ mass of $\pm 0.14 \text{ MeV}/c^2$ [14], the mass scale uncertainty of $^{+0.19}_{-0.21} \text{ MeV}/c^2$ [15] and the uncertainty in the detector resolution of $\pm 10\%$ as estimated by comparison of the inclusive $\Lambda_c^+ \rightarrow pK^- \pi^+$ signal in data and MC simulation. In the region between the $\Lambda_c(2880)^+$ and $\Lambda_c(2940)^+$ signals the fit is systematically below the data points, which might be due to a presence of an additional resonance or due to interference. We take into account these possibilities as a systematic uncertainty. In each

TABLE I. Signal yield, mass, and width for the $\Lambda_c(2880)^+$ and $\Lambda_c(2940)^+$. The first uncertainty is statistical, the second one systematic.

State	Yield	M (MeV/ c^2)	Γ (MeV)
$\Lambda_c(2880)^+$	690 ± 50	$2881.2 \pm 0.2 \pm 0.4$	$5.8 \pm 0.7 \pm 1.1$
$\Lambda_c(2940)^+$	220^{+80}_{-60}	$2938.0 \pm 1.3^{+2.0}_{-4.0}$	13^{+8+27}_{-5-7}

case we consider the largest positive and negative variation in the $\Lambda_c(2880)^+$ and $\Lambda_c(2940)^+$ parameters to be the systematic uncertainty from this source; each term is then added in quadrature to give the total systematic uncertainty, quoted in Table I. The main sources of the systematic uncertainty are a possible contribution of the $\Lambda_c(2765)^+$ tail into the fit region (the shape of the tail is not well constrained) and the excess of events between the $\Lambda_c(2880)^+$ and $\Lambda_c(2940)^+$ signals. None of the variations in the analysis alters the $\Lambda_c(2940)^+$ signal significance to less than 6.2 standard deviations.

Using MC simulation, we study possible backgrounds from the $\Xi_c(2980)/\Xi_c(3077) \rightarrow \Lambda_c^+ K^- \pi^+$ decays [9], when the K^- is misidentified as the π^- , and from the $\Sigma_c(2800) \rightarrow \Lambda_c^+ \pi$ decays [8], when an additional pion is combined with the Λ_c^+ to form a false $\Sigma_c(2455)$. The contributions of these backgrounds are found to be negligible.

For further analysis, we remove the $\cos\theta > 0$ requirement. To study the resonant structure of the $\Lambda_c(2880)^+ \rightarrow \Lambda_c^+ \pi^+ \pi^-$ decays we fit the $\Lambda_c^+ \pi^+ \pi^-$ mass spectrum in $M(\Lambda_c^+ \pi^\pm)$ bins. By isospin symmetry, we expect equally many decays to proceed via a doubly charged $\Sigma_c(2455)$ [$\Sigma_c(2520)$] as via a neutral one. Since the corresponding doubly charged and neutral channels are kinematically separated in phase space, we combine the $M(\Lambda_c^+ \pi^+ \pi^-)$ distributions for $M(\Lambda_c^+ \pi^-)$ and $M(\Lambda_c^+ \pi^+)$ bins. To fit the $\Lambda_c^+ \pi^+ \pi^-$ mass spectra we use the same fit function as described above. The $\Lambda_c(2880)^+$ and $\Lambda_c(2940)^+$ parameters are fixed to the values in Table I. The $\Lambda_c(2880)^+$ yield as a function of $M(\Lambda_c^+ \pi^\pm)$ is shown in Fig. 2. We find a

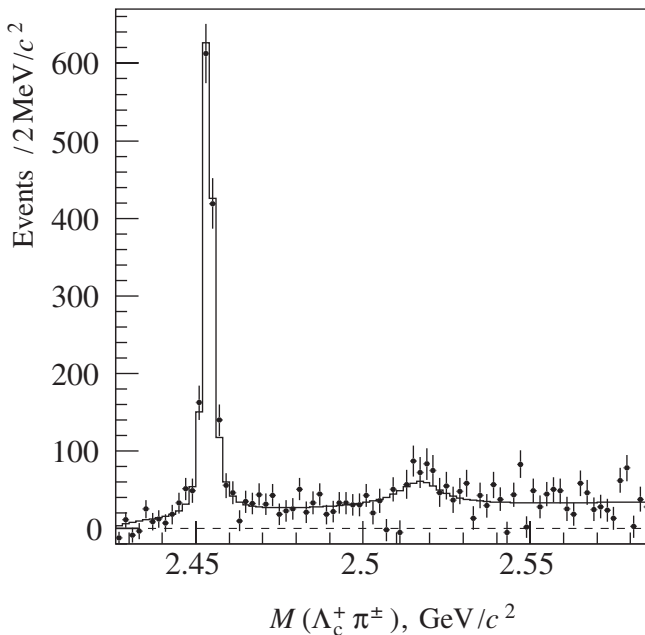


FIG. 2. The $\Lambda_c(2880)^+$ yield as a function of $M(\Lambda_c^+ \pi^\pm)$. The histogram represents the result of the fit.

clear signal for the $\Sigma_c(2455)$ and an excess of events in the region of the $\Sigma_c(2520)$. We perform a χ^2 fit to the $\Lambda_c^+ \pi^\pm$ mass spectrum of Fig. 2 to extract the yields of the $\Sigma_c(2455)$ and $\Sigma_c(2520)$. The fitting function is a sum of three components: $\Sigma_c(2455)$ signal, $\Sigma_c(2520)$ signal, and a nonresonant contribution. The $\Sigma_c(2455)$ and $\Sigma_c(2520)$ signals are parametrized by a P -wave Breit-Wigner function convolved with the detector resolution functions, determined from MC simulation [$\sigma = 0.9$ MeV/ c^2 for the $\Sigma_c(2455)$ and $\sigma = 1.5$ MeV/ c^2 for the $\Sigma_c(2520)$]. The mass and width of the $\Sigma_c(2455)$ are floated, while the mass and width of the $\Sigma_c(2520)$ are fixed to the world average values [5]. The shape of the nonresonant contribution is determined from MC simulation assuming a uniform distribution of the signal over phase space. In this and all the following fits we use the function value averaged over the bin. The fit is shown in Fig. 2. We find the ratios of $\Lambda_c(2880)^+$ partial widths $\Gamma(\Sigma_c(2455)\pi^\pm)/\Gamma(\Lambda_c^+ \pi^+ \pi^-) = 0.404 \pm 0.021 \pm 0.014$, $\Gamma(\Sigma_c(2520)\pi^\pm)/\Gamma(\Lambda_c^+ \pi^+ \pi^-) = 0.091 \pm 0.025 \pm 0.010$, and $\Gamma(\Sigma_c(2520)\pi^\pm)/\Gamma(\Sigma_c(2455)\pi^\pm) = 0.225 \pm 0.062 \pm 0.025$, where the uncertainties are statistical and systematic, respectively. The $\Sigma_c(2455)$ parameters determined from the fit $M = (2453.7 \pm 0.1)$ MeV/ c^2 and $\Gamma = (2.0 \pm 0.2)$ MeV are consistent with the world average values [5]. The normalized χ^2 of the fit is $\chi^2/\text{d.o.f.} = 106.6/75$ (probability 1.0%). The significance of the $\Sigma_c(2520)$ signal is 3.7 standard deviations. The significance is calculated using the same method that was applied to the $\Lambda_c(2940)^+$.

To estimate the systematic uncertainties on the ratios of $\Lambda_c(2880)^+$ partial widths, we vary the $\Lambda_c(2880)^+$ parameters, fit interval, and background parametrization in the fit to the $M(\Lambda_c^+ \pi^+ \pi^-)$ spectrum; we vary the $\Sigma_c(2520)$ parameters; we allow the shape of the nonresonant contribution to float in the fit, parametrizing it with a second-order polynomial multiplied by a threshold function or by a third-order polynomial; we take into account the uncertainty in the detector resolution and in the reconstruction efficiency. None of the variations reduces the significance of the $\Sigma_c(2520)$ signal below 3 standard deviations.

To perform angular analysis of $\Lambda_c(2880)^+ \rightarrow \Sigma_c(2455)^{0,++} \pi^{+,-}$ decays we fit the $\Lambda_c^+ \pi^+ \pi^-$ spectrum in $\cos\theta$ and ϕ bins for the $\Sigma_c(2455)$ signal region and sidebands. Here, ϕ is the angle between the $e^+e^- \rightarrow \Lambda_c(2880)^+ X$ reaction plane and the plane defined by the pion momentum and the $\Lambda_c(2880)^+$ boost direction in the rest frame of the $\Lambda_c(2880)^+$. Figure 3 shows the yield of $\Lambda_c(2880)^+$ as a function of $\cos\theta$ and ϕ , after $\Sigma_c(2455)$ sideband subtraction (to account for nonresonant $\Lambda_c^+ \pi^+ \pi^-$ decays) and efficiency correction.

The parametrization of $\Lambda_c(2880)^+ \rightarrow \Sigma_c(2455)\pi$ decay angular distributions depends on the spin of the $\Lambda_c(2880)^+$. For the spin $\frac{1}{2}$ hypothesis both $\cos\theta$ and ϕ distributions are expected to be uniform [16]. χ^2 fits to a constant are shown in Fig. 3 by a dotted line. The agree-

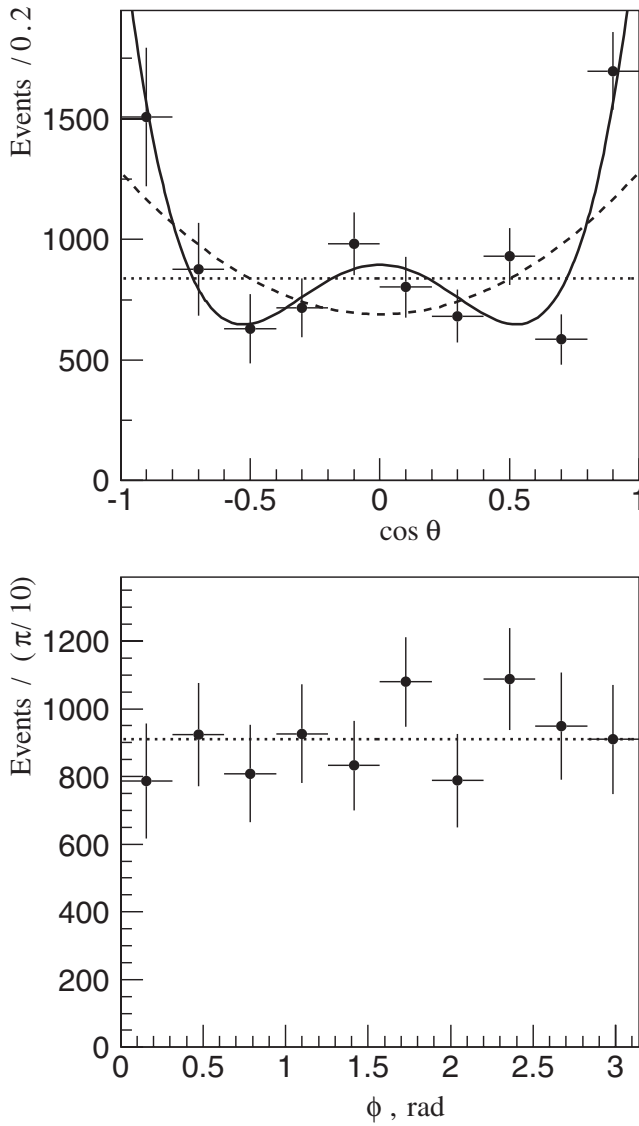


FIG. 3. The yield of $\Lambda_c(2880)^+ \rightarrow \Sigma_c(2455)^{0,++} \pi^{+,-}$ decays as a function of $\cos\theta$ and ϕ . The fits are described in the text.

ment is good for ϕ : $\chi^2/\text{d.o.f.} = 5.3/9$ (probability 81%), but poor for $\cos\theta$: $\chi^2/\text{d.o.f.} = 46.7/9$ (probability 4.5×10^{-7}).

The angular distribution for the spin $\frac{3}{2}$ hypothesis is [16]

$$W_{3/2} = \frac{3}{4\pi} \left[\rho_{33} \sin^2\theta + \rho_{11} \left(\frac{1}{3} + \cos^2\theta \right) - \frac{2}{\sqrt{3}} \text{Re}\rho_{3-1} \sin^2\theta \cos 2\phi - \frac{2}{\sqrt{3}} \text{Re}\rho_{31} \sin 2\theta \cos\phi \right],$$

where ρ_{ij} are the elements of the production density matrix. The diagonal elements are real and satisfy $2(\rho_{33} + \rho_{11}) = 1$. Since the measured distribution in ϕ is consistent with being uniform (this also holds separately for

$\cos\theta > 0$ and $\cos\theta < 0$ samples), the nondiagonal elements are small. The result of the fit to the $\cos\theta$ spectrum for the spin $\frac{3}{2}$ hypothesis is shown in Fig. 3 with a dashed curve. The agreement is poor: $\chi^2/\text{d.o.f.} = 35.1/8$ (probability 2.6×10^{-5}).

The angular distribution for the spin $\frac{5}{2}$ hypothesis is [16]

$$W_{5/2} = \frac{3}{8} [\rho_{55} 2(5\cos^4\theta - 2\cos^2\theta + 1) + \rho_{33}(-15\cos^4\theta + 14\cos^2\theta + 1) + \rho_{11} 5(1 - \cos^2\theta)^2],$$

where nondiagonal elements are ignored. The result of the fit to the $\cos\theta$ spectrum for the spin $\frac{5}{2}$ hypothesis is shown in Fig. 3 with a solid curve. The agreement is good: $\chi^2/\text{d.o.f.} = 12.2/7$ (probability 9.4%). We find $\rho_{55} = 0.088 \pm 0.024$ and $\rho_{33} = 0.00 \pm 0.03$. Thus the $\Lambda_c(2880)^+$ populates mainly the helicity $\pm\frac{1}{2}$ states, $2\rho_{11} = 1 - 2\rho_{33} - 2\rho_{55} = 0.82 \pm 0.08$.

The χ^2 difference of the spin $\frac{1}{2}$ ($\frac{3}{2}$) and spin $\frac{5}{2}$ fits is distributed as χ^2 with two degrees (one degree) of freedom; therefore, the spin $\frac{5}{2}$ hypothesis is favored over the spin $\frac{1}{2}$ ($\frac{3}{2}$) hypothesis at the level of 5.5 (4.8) standard deviations.

To estimate the systematic uncertainty in the angular analysis of the $\Lambda_c(2880)^+ \rightarrow \Sigma_c(2455)^{0,++} \pi^{+,-}$ decay we vary the $\Lambda_c(2880)^+$ parameters, fit interval, and background parametrization in the fit to the $M(\Lambda_c^+ \pi^+ \pi^-)$ spectrum. For all variations the spin $\frac{5}{2}$ hypothesis is favored over the spin $\frac{1}{2}$ ($\frac{3}{2}$) hypothesis at the level of more than 5.4 (4.5) standard deviations.

The Capstick-Isgur quark model predicts the lowest $J^P = \frac{5}{2}^- \Lambda_c^+$ state at 2900 MeV/ c^2 and the lowest $J^P = \frac{5}{2}^+ \Lambda_c^+$ state at 2910 MeV/ c^2 [1]. The typical accuracy of quark model predictions is 50 MeV/ c^2 ; therefore, the agreement with the experimental value for the $\Lambda_c(2880)^+$ mass is quite good. The lowest spin $\frac{5}{2}$ states are well separated from the next $J = \frac{5}{2}$ levels (3130 MeV/ c^2 for negative and 3140 MeV/ c^2 for positive parities) and from $J = \frac{7}{2}$ levels (3125 MeV/ c^2 for negative and 3175 MeV/ c^2 for positive parities).

Heavy quark symmetry predicts $R \equiv \Gamma(\Sigma_c(2520)\pi)/\Gamma(\Sigma_c(2455)\pi) = 1.4$ for the $\frac{5}{2}^-$ state and $R = 0.23 - 0.36$ for the $\frac{5}{2}^+$ state [2,17]. The measured value $R = 0.225 \pm 0.062 \pm 0.025$ favors the positive parity assignment for the $\Lambda_c(2880)^+$.

The $\frac{5}{2}^+$ assignment for the $\Lambda_c(2880)^+$ makes it a special state that lies on the leading Λ_c^+ Regge trajectory, whose lower J^P members are the $\frac{1}{2}^+ \Lambda_c^+$ and $\frac{3}{2}^- \Lambda_c(2625)^+$. The $\frac{5}{2}^+$ assignment for the $\Lambda_c(2880)^+$ based on a string model for baryons was proposed in Ref. [18].

In summary, from angular analysis of $\Lambda_c(2880)^+ \rightarrow \Sigma_c(2455)^{0,++} \pi^{+,-}$ decays we find that a $\Lambda_c(2880)^+$ spin hypothesis of $\frac{5}{2}$ is strongly favored over $\frac{1}{2}$ and $\frac{3}{2}$. We

find first evidence for $\Sigma_c(2520)\pi$ intermediate states in the $\Lambda_c(2880)^+ \rightarrow \Lambda_c^+ \pi^+ \pi^-$ decays and measure $\Gamma(\Sigma_c(2520)\pi^\pm)/\Gamma(\Sigma_c(2455)\pi^\pm) = 0.225 \pm 0.062 \pm 0.025$. This value is in agreement with heavy quark symmetry predictions and favors the $\frac{5}{2}^+$ over the $\frac{5}{2}^-$ hypothesis for the spin-parity of the $\Lambda_c(2880)^+$. We also report the first observation of $\Lambda_c(2940)^+ \rightarrow \Sigma_c(2455)\pi$ decays, and measure the $\Lambda_c(2880)^+$ and $\Lambda_c(2940)^+$ parameters.

We are grateful to A. Kaidalov, I. Klebanov, and Yu. Simonov for valuable discussions. We thank the KEKB group for excellent operation of the accelerator, the KEK cryogenics group for efficient solenoid operations, and the KEK computer group and the NII for valuable computing and Super-SINET network support. We acknowledge support from MEXT and JSPS (Japan), ARC and DEST (Australia), NSFC and KIP of CAS (China), DST (India), MOEHRD, KOSEF, and KRF (Korea), KBN (Poland), MIST (Russia), ARRS (Slovenia), SNSF (Switzerland), NSC and MOE (Taiwan), and DOE (USA).

-
- [1] S. Capstick and N. Isgur, Phys. Rev. D **34**, 2809 (1986).
 - [2] N. Isgur and M. B. Wise, Phys. Rev. Lett. **66**, 1130 (1991).
 - [3] Y. Oh and B. Y. Park, Phys. Rev. D **53**, 1605 (1996).
 - [4] S. Migura, D. Merten, B. Metsch, and H. R. Petry, Eur. Phys. J. A **28**, 41 (2006).

- [5] W.-M. Yao *et al.* (Particle Data Group), J. Phys. G **33**, 1 (2006).
- [6] B. Aubert *et al.* (BABAR Collaboration), Phys. Rev. Lett. **97**, 232001 (2006).
- [7] M. Artuso *et al.* (CLEO Collaboration), Phys. Rev. Lett. **86**, 4479 (2001).
- [8] R. Mizuk *et al.* (Belle Collaboration), Phys. Rev. Lett. **94**, 122002 (2005).
- [9] R. Chistov *et al.* (Belle Collaboration), Phys. Rev. Lett. **97**, 162001 (2006).
- [10] B. Aubert *et al.* (BABAR Collaboration), Phys. Rev. Lett. **98**, 012001 (2007).
- [11] S. Kurokawa and E. Kikutani, Nucl. Instrum. Methods Phys. Res., Sect. A **499**, 1 (2003), and other papers included in this volume.
- [12] A. Abashian *et al.* (Belle Collaboration), Nucl. Instrum. Methods Phys. Res., Sect. A **479**, 117 (2002).
- [13] R. Brun *et al.*, GEANT 3.21, CERN Report No. DD/EE/84-1, 1984.
- [14] B. Aubert *et al.* (BABAR Collaboration), Phys. Rev. D **72**, 052006 (2005).
- [15] K. Abe *et al.* (Belle Collaboration), arXiv:hep-ex/0608012.
- [16] H. M. Pilkuhn, *The Interactions of Hadrons* (North-Holland, Amsterdam, 1967). We assume the J^P of the well established $\Sigma_c(2455)$ to be $\frac{1}{2}^+$.
- [17] H. Y. Cheng and C. K. Chua, Phys. Rev. D **75**, 014006 (2007).
- [18] A. Selem and F. Wilczek, arXiv:hep-ph/0602128; I. Klebanov (private communication).